770 *Biochemistry* **2011,** *50,* 770–779
DOI: 10.1021/bi101837u

BIOCHEMISTRY
including biophysical chemistry & molecular biology
Article

Importance of a Serine Proximal to the C(4a) and N(5) Flavin Atoms for Hydride Transfer in Choline Oxidase[†]

Hongling Yuan[‡] and Giovanni Gadda*[,‡,§,∥]

[‡]*Department of Chemistry,* [§]*Department of Biology, and* [∥]*The Center for Biotechnology and Drug Design, Georgia State University, Atlanta, Georgia 30302-4098, United States*

Received November 17, 2010; Revised Manuscript Received December 15, 2010

ABSTRACT: Choline oxidase catalyzes the flavin-dependent, two-step oxidation of choline to glycine betaine with the formation of an aldehyde intermediate. In the first oxidation reaction, the alcohol substrate is initially activated to its alkoxide via proton abstraction. The substrate is oxidized via transfer of a hydride from the alkoxide α-carbon to the N(5) atom of the enzyme-bound flavin. In the wild-type enzyme, proton and hydride transfers are mechanistically and kinetically uncoupled. In this study, we have mutagenized an active site serine proximal to the C(4a) and N(5) atoms of the flavin and investigated the reactions of proton and hydride transfers by using substrate and solvent kinetic isotope effects. Replacement of Ser101 with threonine, alanine, cysteine, or valine resulted in biphasic traces in anaerobic reductions of the flavin with choline investigated in a stopped-flow spectrophotometer. Kinetic isotope effects established that the kinetic phases correspond to the proton and hydride transfer reactions catalyzed by the enzyme. Upon removal of Ser101, there is an at least 15-fold decrease in the rate constants for proton abstraction, irrespective of whether threonine, alanine, valine, or cysteine is present in the mutant enzyme. A logarithmic decrease spanning 4 orders of magnitude is seen in the rate constants for hydride transfer with increasing hydrophobicity of the side chain at position 101. This study shows that the hydrophilic character of a serine residue proximal to the C(4a) and N(5) flavin atoms is important for efficient hydride transfer.

Choline oxidase (EC 1.1.3.17, choline-oxygen 1-oxidoreductase) catalyzes the flavin-mediated oxidation of choline to glycine betaine (*1*). This reaction is of considerable interest for medical and biotechnological applications because the intracellular accumulation of glycine betaine, a compatible solute that does not interfere with cytoplasmic function at high concentrations, is important for normal cell function under conditions of osmotic and temperature stress in bacteria and plants (*2*−*5*). Furthermore, glycine betaine is much more effective than other compatible solutes in the stabilization of the structure and function of macromolecules and the highly ordered state of membranes (*6*). In biotechnology, the *codA* gene encoding choline oxidase is used to improve the tolerance of economically important crops like tomatoes, potatoes, and rice toward environmental stresses because of the hypersalinity of the soil or high and low temperatures (*7*−*9*). A membrane-associated choline dehydrogenase that is homologous to the cytosolic oxidase is found in many pathogenic bacteria, where it was recently shown that the *betA* gene encoding the dehydrogenase is likely associated with virulence (*10*). Thus, the study of the mechanism of choline oxidase offers an opportunity to control glycine betaine biosynthesis in pathogenic bacteria and to provide osmotic balance with the environment in plants.

Choline oxidase from *Arthrobacter globiformis* has been investigated using biophysical (*11*−*14*), structural (*15*, *16*), mechanistic (*17*−*24*), computational (*25*), and site-directed mutagenic (*13*, *15*, *26*−*34*) approaches. The reaction of choline oxidation catalyzed by choline oxidase includes two reductive half-reactions in which the FAD cofactor is reduced in subsequent steps by the alcohol substrate and an aldehyde intermediate of the reaction. Each reductive half-reaction is followed by an oxidative half-reaction in which the reduced FAD cofactor is oxidized by molecular oxygen with formation of hydrogen peroxide (Scheme 1) (for a recent review, see ref *1*). In the wild-type enzyme, the first oxidation is triggered by the kinetically fast abstraction of the hydroxyl proton of choline by a catalytic base with a pK_a of ∼7.5, which has not yet been identified (*27*, *29*, *34*), resulting in the formation of a transient alkoxide (*11*, *17*, *19*, *20*, *24*). The side chains of His351 and His466 contribute to the stabilization of the alkoxide species through hydrogen bonding and electrostatic interactions, respectively (*29*, *34*). A rate-limiting transfer of a hydride ion from the α-carbon of the alkoxide species to the N(5) atom of the flavin results in the oxidation of choline and the reduction of the enzyme-bound flavin. This was established with solvent, substrate, and multiple kinetic isotope effects on the steady state kinetic parameter k_{cat}/K_m with choline as a substrate for the enzyme (*1*, *20*). The abstraction of the hydroxyl proton of the substrate is associated with an isomerization of the enzyme−substrate complex that is kinetically independent of the subsequent reaction of hydride ion transfer. This is suggested in the wild-type enzyme by the comparison of the kinetic isotope effects on the flavin reduction step under reversible and irreversible catalytic regimes (*24*), and in active site mutant enzymes with replacements of residues that are not directly involved in catalysis, namely, Glu312 with aspartate or Val464 with either alanine or threonine, by substrate or solvent kinetic isotope effects (*15*, *31*).

[†]This work was supported in part by NSF-CAREER Grant MCB-0545712 (to G.G.).

*To whom correspondence should be addressed: Department of Chemistry, Georgia State University, P.O. Box 4098, Atlanta, GA 30302-4098. Phone: (404) 413-5537. Fax: (404) 413-5505. E-mail: ggadda@gsu.edu.

 Published on Web 12/21/2010

Scheme 1: Two-Step Oxidation of Choline Catalyzed by Choline Oxidase

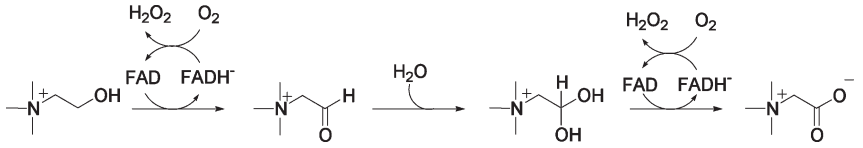

In the X-ray structure of choline oxidase resolved to 1.86 Å, the Oγ atom of Ser101 is less than 4 Å from the N(5) atom of FAD and within hydrogen bonding distance (i.e., < 3 Å) of the oxygen atom of DMSO[1] (Figure 1), an additive that was used in the crystallization of the enzyme (*15*). This suggests that Ser101 may interact with the substrate and be actively involved in the oxidation of choline catalyzed by the enzyme. Moreover, the recent determination of the X-ray structure of the Ser101Ala enzyme to a resolution of 2.5 Å showed a lack of structural changes in the active site and the overall structure of the enzyme upon replacement of the side chain on residue 101 (Figure 1) (*33*). This prompted us to investigate the role of Ser101 in the reductive half-reaction catalyzed by choline oxidase by using site-directed mutagenesis and rapid kinetics.

In this study, the effects of replacing Ser101 with alanine, threonine, cysteine, or valine on the reductive half-reaction catalyzed by choline oxidase have been investigated using both solvent and substrate kinetic isotope effects in a stopped-flow spectrophotometer. The mutated enzymes were slower than the wild-type enzyme in their ability to activate choline to the alkoxide species, resulting in biphasic reductions of the flavin in anaerobic stopped-flow reactions with choline. Kinetic isotope effects allowed us to assign the two kinetic phases of flavin reduction to the stepwise cleavages of the substrate O−H and C−H bonds. Finally, it was shown that the rate of transfer of the hydride ion from the alkoxide to the flavin decreased with the decreasing hydrophilicity of the side chain of residue 101.

EXPERIMENTAL PROCEDURES

Materials. *Escherichia coli* strain Rosetta(DE3)pLysS was from Novagen (Madison, WI). The QIAprep Spin Miniprep kit was from Qiagen (Valencia, CA). The QuickChange site-directed mutagenesis kit was from Stratagene (La Jolla, CA). Oligonucleotides for site-directed mutagenesis and sequencing of the mutant genes were from Sigma Genosys (The Woodlands, TX). 1,2-[$^2H_4$]Choline and sodium deuterium oxide (99%) were from Isotec Inc. (Miamisburg, OH). Polyethylene glycol 6000 was from Fluka (St. Louis, MO). Choline chloride was from ICN Pharmaceutical Inc. (Irvine, CA). All other reagents used were of the highest purity commercially available.

Instruments. UV−visible absorbance spectra were recorded using an Agilent Technologies model HP 8453 diode array spectrophotometer equipped with a thermostated water bath. The enzymatic activity of choline oxidase was measured polarographically using a computer-interfaced Oxy-32 oxygen monitoring system (Hansatech Instrument Ltd.). Stopped-flow experiments were conducted using a Hi-Tech SF-61 double-mixing stopped-flow spectrophotometer.

[1]Abbreviations: Ser101Ala enzyme, choline oxidase in which Ser101 is substituted with alanine; Ser101Thr enzyme, choline oxidase in which Ser101 is substituted with threonine; Ser101Val enzyme, choline oxidase in which Ser101 is substituted with valine; Ser101Cys enzyme, choline oxidase in which Ser101 is substituted with cysteine; Asn510His enzyme, choline oxidase in which Asn510 is substituted with histidine; DMSO, dimethyl sulfoxide; KIE, kinetic isotope effect.

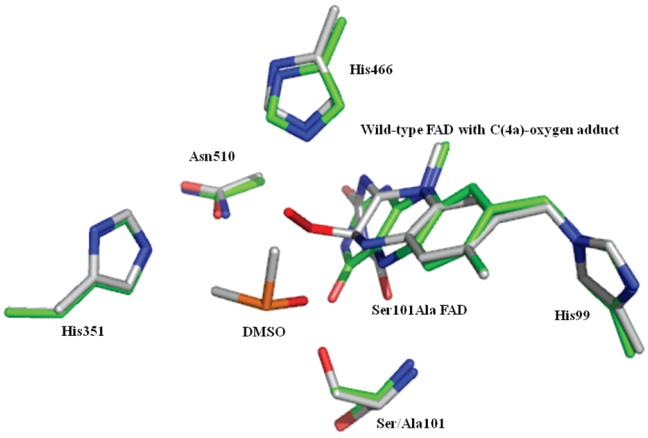

FIGURE 1: Comparison of the active sites of wild-type and Ser101Ala choline oxidase. The residues with carbons colored green represent the mutant structure, whereas the carbon atoms for the wild-type enzyme are colored gray. The C(4a)−oxygen adduct observed with the wild-type enzyme is colored red. The structures of the wild-type and S101A mutant enzymes are from Protein Data Bank entries 2JBV (*15*) and 3NNE (*33*), respectively.

Site-Directed Mutagenesis and Protein Purification. The mutated genes for the choline oxidase variants containing alanine, threonine, cysteine, or valine instead of Ser101 were prepared as previously described (*12*). The resulting mutant genes were sequenced at the DNA Core Facility of Georgia State University using an Applied Biosystems Big Dye Kit on an Applied Biosystems model ABI 377 DNA sequencer to confirm the presence of the mutation. The mutant enzymes were expressed and purified to homogeneity as previously described for wild-type choline oxidase (*12*, *13*, *19*). The enzymes were stored at −20 °C in 20 mM Tris-HCl (pH 8.0) and were found to be stable for at least 6 months.

Kinetic Assays. The apparent steady state kinetic parameters in atmospheric oxygen of the mutant enzymes were measured with the method of initial rates by monitoring oxygen consumption as described for wild-type choline oxidase (*20*).

Observed rate constants for flavin reduction of the enzymes were determined anaerobically at varying concentrations of substrate (choline or 1,2-[$^2H_4$]choline) in 50 mM sodium pyrophosphate (pH 10.0) using a stopped-flow spectrophotometer thermostated at 25 °C, as previously described (*15*). Equal volumes of the enzyme and substrate were mixed anaerobically in the stopped-flow spectrophotometer in the presence of a glucose (5 mM)/glucose oxidase (0.5 μM) mixture, yielding a final enzyme concentration of ~10 μM. Substrate concentrations were ≥50 μM, ensuring pseudo-first-order conditions. Data were collected in the dual beam mode using photomultiplier detection set at 452 nm.

For the determination of solvent kinetic isotope effects on the observed first-order rate constants for flavin reduction, all of the reagents were prepared using 99.9% deuterium oxide by adjusting the pD value with NaOD. The pD values were determined by addition of 0.4 to the pH electrode readings (*35*). Solvent viscosity

Table 1: Comparison of Spectral and Catalytic Properties of Ser101 Mutant Enzymes and Wild-Type Choline Oxidase

	λ_{max} (nm)[b]	ε (mM^{-1} cm^{-1})	$^{app}(k_{cat}/K_m)$ (M^{-1} s^{-1})	$^{app}k_{cat}$ (s^{-1})	$^{app}K_m$ (mM)
wild type[a]	367, 455	10, 11.4	25000	15	0.6
Ser101Thr	371, 450	8.7, 9.3	18000 ± 2000	3.0 ± 0.1	0.17 ± 0.02
Ser101Ala	373, 452	8.9, 9.5	4600 ± 400	3.3 ± 0.1	0.73 ± 0.07
Ser101Cys	374, 450	9.2, 9.9	1100 ± 70	0.076 ± 0.001	0.07 ± 0.01
Ser101Val	371, 452	9.2, 10.9	21 ± 1	0.017 ± 0.001	0.82 ± 0.03

[a]From ref *15*. [b]Absorbance spectra were recorded at pH 8.0 and 25 °C. Enzymatic activities were measured in 50 mM potassium phosphate (pH 7.0) at 25 °C, using fully oxidized enzymes.

effects were measured in the presence of 0.0211 g/mL PEG-6000 as the viscosigen (which is equivalent to a relative viscosity of 1.26) (*36*), in both the tonometer containing the enzyme and the syringes containing the organic substrates.

Data Analysis. Kinetic data were fit with KaleidaGraph (Synergy Software, Reading, PA) and the Kinetic Studio Software Suite (Hi-TgK Scientific, Bradford on Avon, U.K.). The apparent steady state kinetic parameters in atmospheric oxygen were determined by fitting the data to the Michaelis−Menten equation for one substrate.

Stopped-flow traces were fit to eq 1, which describes a double-exponential process

$$A = B\exp(-k_{obs1}t) + C\exp(-k_{obs2}t) + D \quad (1)$$

where k_{obs1} and k_{obs2} represent the observed first-order rate constants associated with the absorbance changes of the fast and slow phases, respectively, t is the time, A is the absorbance at 452 nm at any given time, B and C are the amplitudes of the absorbance changes for the fast and slow phases, respectively, and D is the absorbance at infinite time. The kinetic parameters associated with the fast and slow phases of flavin reduction seen in the reductive half-reaction were determined by using eqs 2 and 3, respectively (see the Appendix for derivation).

$$k_{obs1} = \frac{k_{lim1}S + c}{^{app}K_{fast} + S} \quad (2)$$

$$k_{obs2} = \frac{k_{lim2}S}{^{app}K_{slow} + S} \quad (3)$$

where k_{obs1} and k_{obs2} represent the observed first-order rate constants associated with the absorbance changes of the fast and slow phases, respectively, at any given concentration of substrate (S); k_{lim1} and k_{lim2} are the limiting rate constants at a saturated substrate concentration of the fast and slow phases, respectively; $^{app}K_{fast}$ and $^{app}K_{slow}$ are the apparent dissociation constants defining equilibria between the free enzyme and free substrate and enzyme−substrate complexes, respectively; and c is a constant.

RESULTS

Expression and Purification of Ser101 Mutant Enzymes. The choline oxidase variants in which Ser101 is replaced with alanine, threonine, cysteine, or valine were expressed and purified by using the same protocol previously used for the wild-type enzyme (*12*). A mixture of air-stable anionic semiquinone and oxidized flavin species was observed throughout the purification procedure of all the mutant enzymes, as previously reported for the wild-type enzyme (*11*, *12*). The fully oxidized and active mutant enzymes were obtained by dialysis at pH 6.0, following the procedure described for the wild-type enzyme (*12*). In all cases, the flavin was covalently linked to the protein as established by heat denaturation of the mutant enzymes followed by spectroscopic analysis of the samples after removal of the denatured proteins by centrifugation. The spectral properties of the oxidized Ser101 mutant enzymes are summarized in Table 1, along with the apparent steady state kinetic parameters determined with choline at atmospheric oxygen concentrations and pH 7.0. The $^{app}(k_{cat}/K_m)$ and $^{app}k_{cat}$ values of the mutant enzymes were between 1.5- and 1000-fold lower than those of the wild-type enzyme, indicating that Ser101 is an important residue for catalysis in choline oxidase.

Reductive Half-Reaction. The reductive half-reactions of the Ser101Ala, Ser101Thr, Ser101Cys, and Ser101Val enzymes were studied in a stopped-flow spectrophotometer by mixing anaerobic solutions of the enzyme with different concentrations of anaerobic choline at pH 10.0 and 25 °C under pseudo-first-order conditions (i.e., 0.01 mM enzyme and 0.05−5 mM choline). An alkaline pH was chosen because previous results established that catalysis is pH-independent in the wild type and a number of active site mutant enzymes of choline oxidase at pH 10.0 (*11*, *15*, *17*, *20*−*22*, *29*, *34*). The reduction of enzyme-bound oxidized FAD was monitored by the changes in absorbance at 452 nm. With all enzymes, two kinetic phases were observed (Figure 2A). Full reduction of the enzyme-bound flavin to the anionic hydroquinone species was observed at the end of the slow kinetic phase with all the mutant enzymes and at all substrate concentrations tested, as illustrated in the example of Figure 2B for the Ser101Ala enzyme. In agreement with a biphasic process for the decrease in absorbance at 452 nm, the stopped-flow traces with all of the mutant enzymes were fit best to eq 1, which describes a double-exponential process. When the observed first-order rate constants for the fast (k_{obs1}) and slow (k_{obs2}) phases were plotted as a function of choline concentrations, they both exhibited saturation kinetics (Figure 2C shows the example of the Ser101Ala enzyme). Accordingly, the associated kinetic parameters for the reductive half-reactions of the mutant enzymes were determined by using eqs 2 and 3 (see the Appendix for derivations). With all of the mutant enzymes, the fits of the rapid kinetic data yielded $^{app}K_{fast}$ and $^{app}K_{slow}$ values that were lower than the lowest concentration of choline that could be used to maintain pseudo-first-order conditions (data not shown), thereby preventing accurate determinations of these kinetic parameters. In contrast, accurate determinations of the limiting rate constants at saturated substrate concentrations for the two phases seen in the stopped-flow traces (k_{lim1} and k_{lim2}) could be attained. As summarized in Table 2, the k_{lim1} values for all of the Ser101 mutant enzymes were between 40 and 125 s^{-1}. In contrast, the k_{lim2} values spanned more than 2 orders of magnitude between 0.016 and 6.6 s^{-1}: Thr101 ≈ Ala101 > Cys101 > Val101 (Table 2).

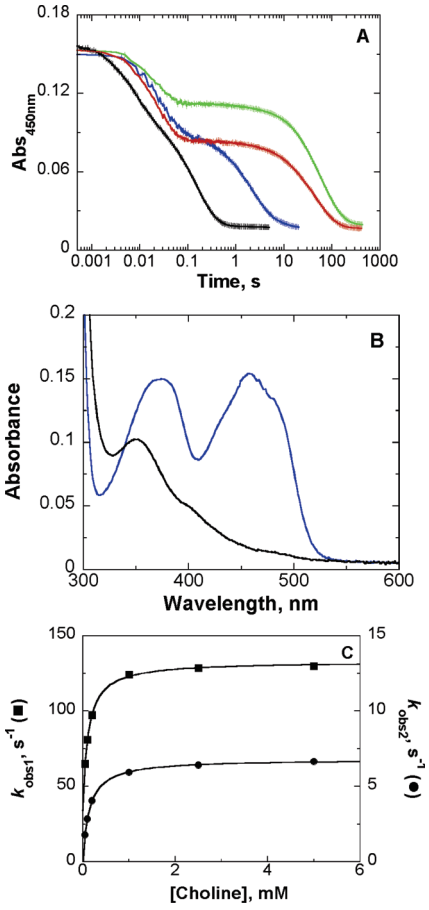

FIGURE 2: Anaerobic reduction of the Ser101 variants with choline as a substrate in 50 mM sodium pyrophosphate (pH 10.0) at 25 °C. (A) Reduction traces with saturating choline for the Ser101Ala (5 mM choline, black curve), Ser101Thr (5 mM choline, blue curve), Ser101Cys (10 mM choline, red curve), and Ser101Val (10 mM choline, green curve) enzymes. All traces were fit with eq 1. The time indicated is after the end of the flow, i.e., 2.2 ms. For the sake of clarity, one experimental point of every five is shown (vertical lines). (B) UV−visible absorbance spectra of the oxidized enzyme (blue) and reduced (black) species of the Ser101Ala enzyme obtained by mixing anaerobically the oxidized enzyme with buffer and 5 mM choline in 50 mM sodium pyrophosphate buffer (pH 10.0) at 25 °C. (C) Observed rate constants for the fast and slow kinetic phases as a function of choline concentration for the Ser101Ala enzyme. Data were fit to eqs 2 and 3 for the fast and slow phases, respectively.

For comparison, the reductive half-reaction with the wild-type enzyme was previously shown to be monophasic with a limiting rate constant for flavin reduction of 93 s^{-1} (*20*).

Substrate Deuterium KIE. Substrate KIEs were used to probe whether the cleavage of the C−H bond of choline is associated with either the fast or the slow kinetic phase observed in the stopped-flow spectrophotometer with the Ser101 mutant enzymes. The Ser101Val enzyme was too slow for an accurate determination of the KIE and was not investigated further. As exemplified in Figure 3 for the Ser101Ala enzyme, substitution of choline with 1,2-[$^2H_4$]choline further slowed the slow kinetic phase observed in the stopped-flow spectrophotometer with all of the Ser101 mutant enzymes. In contrast, there were no significant changes in the fast phases for any of the mutant enzymes (Figure 3A shows the Ser101Ala enzyme as an example). Consequently, significant decreases in the k_{lim2} values were observed, whereas the k_{lim1} values were minimally affected by the substitution of choline with 1,2-[$^2H_4$]choline (Table 2). Accordingly, small

Table 2: Limiting Rate Constants for the Fast and Slow Kinetic Phases of Flavin Reduction with Choline and 1,2-[$^2H_4$]Choline as the Substrate for Ser101 Mutant Enzymes[a]

	k_{lim1} (s^{-1}) (k_3)	k_{lim2} (s^{-1}) (k_5)
	Choline	
Ser101Thr	41 ± 1	3.07 ± 0.05
Ser101Ala	125 ± 2	6.6 ± 0.1
Ser101Cys	47 ± 1	0.10 ± 0.01
Ser101Val	49 ± 1	0.016 ± 0.001
wild type	no[b]	93 ± 1
	1,2-[$^2H_4$]Choline	
Ser101Thr	36 ± 1	0.48 ± 0.02
Ser101Ala	125 ± 6	1.02 ± 0.02
Ser101Cys	44 ± 1	0.020 ± 0.001
wild type	no[b]	10.3 ± 0.3

[a]Determined in 50 mM sodium pyrophosphate (pH 10.0) at 25 °C. [b]Not observed.

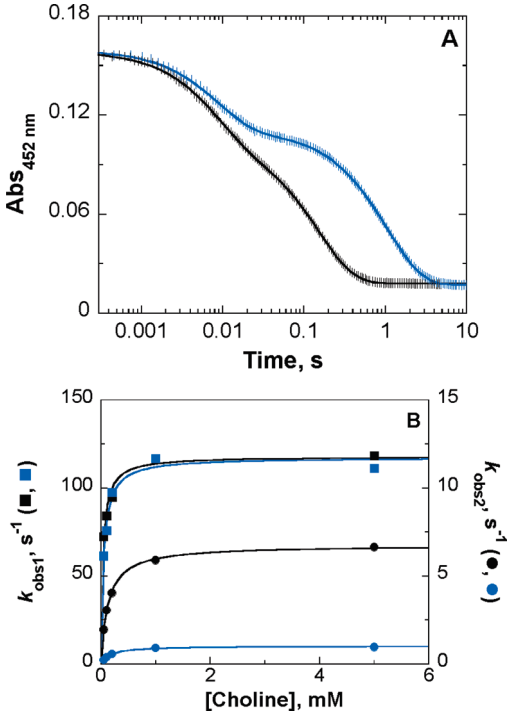

FIGURE 3: Anaerobic substrate reduction of the Ser101Ala enzyme with choline (black) and 1,2-[$^2H_4$]choline (blue) as substrates. The experiments were conducted in 50 mM sodium pyrophosphate (pH 10.0) at 25 °C. (A) Stopped-flow traces at saturating substrate concentrations. All traces were fit with eq 1. The time indicated is after the end of the flow, i.e., 2.2 ms. For the sake of clarity, one experimental point of every five is shown (vertical lines). (B) Observed rate constants for the fast and slow kinetic phases as a function of substrate concentration. Data were fit to eqs 2 and 3 for the fast phase and slow phases, respectively.

substrate KIEs of ≤1.1 were associated with the k_{lim1} values determined with the Ser101Thr, -Ala, and -Cys enzymes, whereas large substrate KIEs between 5.0 and 6.5 were associated with the k_{lim2} values. These results establish the slow kinetic phase of flavin reduction as being primarily due to the cleavage of the substrate C−H bond.

Solvent KIE. Solvent KIEs were used with the Ser101Ala enzyme to probe whether the cleavage of the O−H bond of

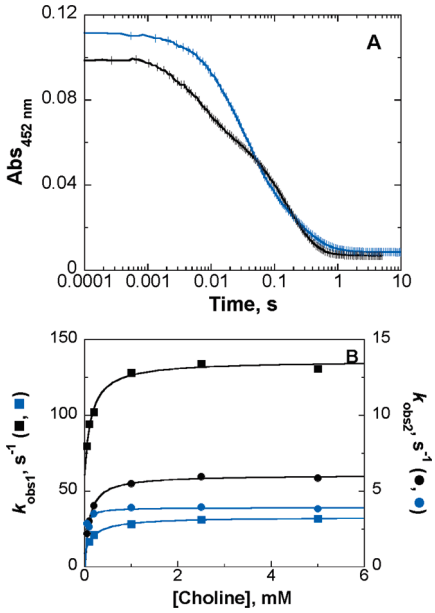

FIGURE 4: Anaerobic substrate reduction of the Ser101Ala enzyme with choline as the substrate in H_2O (black) and D_2O (blue). The experiments were conducted in 50 mM sodium pyrophosphate (pH 10) at 25 °C. (A) Stopped-flow traces at saturating substrate concentrations. The curves were fit to eq 1. The time indicated is after the end of the flow, i.e., 2.2 ms. For the sake of clarity, one experimental point of every five is shown (vertical lines). (B) Observed rate constants for the fast and slow kinetic phases as a function of substrate concentration. Data were fit to eqs 2 and 3 for the fast and slow phases, respectively.

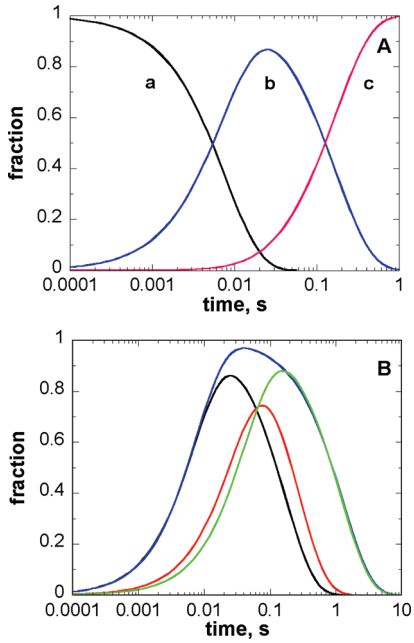

FIGURE 5: Simulated reaction traces with a two-step a → b → c model with equations $A = A_0 \exp(-k_{lim1}t)$, $B = (A_0k_{lim1})/(k_{lim2} - k_{lim1})$-$[\exp(-k_{lim1}t) - \exp(-k_{lim2}t)]$, and $C = A_0\{1 + [k_{lim2} \exp(-k_{lim1}t) - k_{lim1} \exp(-k_{lim2}t)/(k_{lim1} - k_{lim2})]\}$. Kinetic parameters were taken from the experimentally determined values listed in Table 2. (A) Progress curves for the three enzyme−substrate species a (oxidized enzyme−substrate complex), b (transient species), and c (reduced enzyme−product complex) of the Ser101Ala enzyme during anaerobic substrate reduction with 10 mM choline (pH 10.0) at 25 °C. (B) Time courses of species b during reduction in 50 mM sodium pyrophosphate (pH 10.0) with choline in H_2O (black) or D_2O (red) or 1,2-[$^2H_4$]choline in H_2O (blue) or D_2O (green) under anaerobic conditions at 25 °C.

choline is associated with the fast phase observed in the stopped-flow spectrophotometer. When water was substituted with D_2O, there was a significant decrease in the observed rate constants for the fast kinetic phase at 452 nm, with minimal effects on the slow phase (Figure 4). The k_{lim1} and k_{lim2} values determined in D_2O for the Ser101Ala enzyme were 32.8 ± 0.5 and 4.0 ± 0.1 s^{-1}, respectively, yielding solvent KIEs of 3.8 ± 0.1 and 1.65 ± 0.05 for the fast and slow phases, respectively, observed in the stopped-flow spectrophotometer. The effect of increased solvent viscosity on the reductive half-reaction was investigated as a control for the solvent KIE, because D_2O has a relative viscosity of 1.25 at 25 °C. PEG-6000, at a concentration of 0.0211 g/mL that is equivalent to a 100% solution of D_2O, was used in the stopped-flow spectrophotometer. The limiting rate constants at saturating concentrations of choline for both the fast and slow phases were similar to those determined in aqueous solution, yielding $(k_{lim1})_{H_2O}/(k_{lim1})_{PEG}$ and $(k_{lim2})_{H_2O}/(k_{lim2})_{PEG}$ values of 1.05 ± 0.01 and 0.98 ± 0.02, respectively. A lack of solvent viscosity effects establishes the solvent KIEs on the k_{lim1} and k_{lim2} values as being associated with transition states with exchangeable protons being in flight rather than solvent-sensitive equilibria of enzyme−substrate complexes. These data, in turn, are consistent with the fast phase observed in the stopped-flow spectrophotometer being due to the cleavage of the substrate O−H bond.

Kinetic Data Simulation. The two kinetic phases observed in the reductive half-reactions of the Ser101 mutant enzymes are consistent with the minimal kinetic model of eq 4

$$a \leftrightharpoons b \rightleftharpoons c \quad (4)$$

with the oxidized enzyme (a) giving rise to a transient species (b) that eventually decays to the reduced enzyme (c). In eq 4, a and b are reversibly connected to account for the saturation kinetics as a function of substrate concentration that is observed for the slow kinetic phase in the stopped-flow spectrophotometer (*37*). Figure 5A shows the progress curves for the relative amounts of the three species (a, b, and c) that have been generated for the Ser101Ala enzyme using the experimental data with choline (Table 2). Similar time courses show the transient accumulation of the intermediate species b could be generated for the other Ser101 mutant enzymes (data not shown). Simulation of the kinetic data acquired with 1,2-[$^2H_4$]choline in water clearly shows a greater accumulation of the transient species b with respect to the case with choline, as expected because of the similar rates of formation and a slower rate of decay of b when choline is substituted with 1,2-[$^2H_4$]choline (compare the black and blue curves in Figure 5B). Similar accumulation of transient species b, but at a delayed time, is evident in the simulation of the kinetic data with 1,2-[$^2H_4$]-choline in D_2O with respect to those with choline in water, as expected because of the deceleration of the cleavage of both O−H and C−H bonds of the substrate (compare the green and black curves in Figure 5B). Finally, a lower level of accumulation of transient species b is seen in the simulation of the kinetic data with choline in D_2O with respect to water, as expected because of a slower rate of formation and similar rates of decay of b (compare the red and black curves in Figure 5B).

DISCUSSION

The reductive half-reactions of the active site variants of choline oxidase containing alanine, threonine, cysteine, or valine instead of serine at position 101 were investigated to establish the role of

Scheme 2: Proposed Kinetic Mechanism for Reductive Half-Reaction of Ser101 Variants of Choline Oxidase[a]

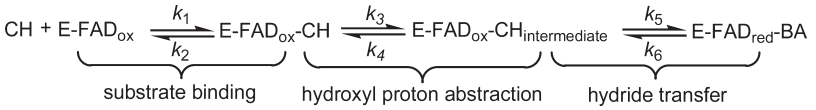

[a]E, enzyme; FAD_{ox}, oxidized flavin; CH, choline; FAD_{red}, reduced flavin; BA, betaine aldehyde.

Ser101 in the reaction of choline oxidation catalyzed by the enzyme. In the case of the Ser101Ala enzyme, the three-dimensional structure of the mutant enzyme was recently shown to be practically identical to that of the wild-type enzyme, with an average root-mean-square deviation (rmsd) of 0.41 Å for 527 equivalent Cα atoms when the structure of the mutant enzyme is overlaid on that of the wild-type enzyme (Figure 1) (*15*, *33*). In this study, we have shown that all of the mutant enzymes shared a number of kinetic, mechanistic, and biochemical properties with the wild-type enzyme. (1) The UV−visible absorbance spectrum had maxima at 367−374 and 450−455 nm in the oxidized state and at 350−360 nm in the hydroquinone state. (2) The flavin was covalently linked to the protein. (3) An anionic flavosemiquinone was aerobically stabilized at pH 8.0 during purification. (4) The substrate KIEs on the limiting rate constant for anaerobic flavin reduction were ≥5.0. This allowed us to compare and contrast the mechanistic properties of the enzymes and to draw conclusions about the role that is played by Ser101 in the activation of the alcohol substrate and the subsequent transfer of a hydride ion from the activated alkoxide to the flavin.

Timing of O−H and C−H Bond Cleavages. The abstraction of the hydroxyl proton of the substrate precedes and is mechanistically independent of the transfer of the hydride ion from the activated substrate to the flavin in the Ser101 mutant enzymes (Scheme 2). Evidence of this conclusion comes from the anaerobic reductive half-reactions with choline of the four variants of choline oxidase substituted at residue 101 and the associated solvent and substrate KIEs. Two kinetic phases, which are well separated from one another, were observed in the stopped-flow traces (Figure 2). A large solvent KIE with a value of ~4 was determined on the k_{lim1} value for the Ser101Ala enzyme, consistent with the fast kinetic phase reflecting the cleavage of the substrate O−H bond. Negligible substrate KIEs of ≤1.1 on the k_{lim1} values and large substrate KIEs of ≥5.0 on the k_{lim2} values were seen with the Ser101Ala, Ser101Thr, and Ser101Cys enzymes, consistent with the slow kinetic phase reflecting the cleavage of the substrate C−H bond.

The analytical equations that define the limiting rate constants at saturating concentrations of choline for the two kinetic phases observed in the stopped-flow traces are given by eqs 5 and 6, with numbering based on Scheme 2 (see the Appendix for derivation).

$$k_{lim1} = k_3 + k_4 + k_5 \quad (5)$$

$$k_{lim2} = \frac{k_3 k_5}{k_3 + k_4 + k_5} \quad (6)$$

These equations simplify further to eqs 7 and 8 because the cleavage of the substrate O−H bond is significantly faster than both its reverse reaction (i.e., $k_3 > k_4$) and the cleavage of the C−H bond (i.e., $k_3 > k_5$).

$$k_{lim1} = k_3 \quad (7)$$

$$k_{lim2} = k_5 \quad (8)$$

The first condition is stipulated by the extrapolation to the origin of the hyperbola fitting the observed rate constants for the fast kinetic phase in the stopped-flow traces as a function of the concentration of choline (Figure 2C). The second condition is indirectly validated by the results of the KIEs; otherwise, both k_{lim1} and k_{lim2} would incorporate both kinetic steps and be sensitive to both substrate and solvent KIEs, as illustrated by eqs 5 and 6. Thus, the timing for the cleavages of the O−H and C−H bonds in the Ser101 mutant enzymes is similar to that of the wild-type choline oxidase (*20*). What is significantly different between the two enzymes is how transition states and reaction intermediates are stabilized in the active site when the serine residue at position 101 is absent or present in the active site (vide infra).

Hydroxyl Proton Abstraction. The hydroxyl group of Ser101 stabilizes the transition state for the abstraction of the hydroxyl proton of choline. Evidence of this conclusion comes from the observation that the substitution of Ser101 with other amino acid residues results in an at least 15-fold decrease in the rate constant for the cleavage of the substrate O−H bond. The fast kinetic phases seen in the stopped-flow traces of the Ser101 mutant enzymes, which report on the cleavage of the substrate O−H bond (vide ante), have limiting rate constants at the saturating choline concentration (k_{lim1}) between 40 and 125 s^{-1}. Instead, cleavage of the substrate O−H bond in the wild-type enzyme has been shown to occur within the dead time of the stopped-flow spectrophotometer (*20*), which corresponds to 2.2 ms. If one considers that six half-lives are required to complete 98.5% of a pseudo-first-order process of the type considered here,[2], a lower limiting value of 1900 s^{-1} can be estimated for the cleavage of the substrate O−H bond in the wild-type choline oxidase. In agreement with substrate O−H bond cleavage occurring during the dead time of the stopped-flow spectrophotometer, previous mechanistic investigations showed that the solvent KIE associated with the anaerobic reduction of the wild-type choline oxidase has a value of 0.99 (*20*). It is likely that in the wild-type enzyme the transition state for the O−H bond cleavage is stabilized by a hydrogen bond involving the side chain of Ser101 and the oxygen atom of the alkoxide species, which is necessarily more electronegative than in the enzyme−substrate complex because of the development of the charged alkoxide intermediate (Scheme 3). In the mutant enzymes containing alanine, valine, and cysteine in place of Ser101, such a transition state stabilization cannot be achieved, thereby making the abstraction of the substrate hydroxyl proton slow. In the case of the Ser101Thr enzyme, a suboptimal geometry of the hydrogen bond due to the presence of the extra methyl may be responsible for the slow rate of proton abstraction.

Hydride Ion Transfer. The hydroxyl group of Ser101 provides a hydrophilic microenvironment with hydrogen bonding

[2]In the four enzymes mutated at Ser101, cleavage of the substrate O−H bond is a first-order process (Figure 2A). It is therefore reasonable to assume that cleavage of the substrate O−H bond by the wild-type enzyme is also a first-order process.

Scheme 3: Roles of Ser101 in the Cleavages of the O−H (a) and C−H (b) Bonds of Choline[a]

a) OH bond cleavage:

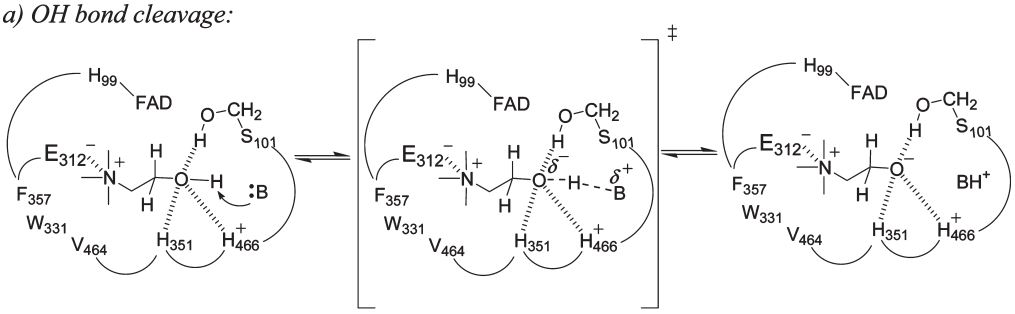

b) CH bond cleavage:

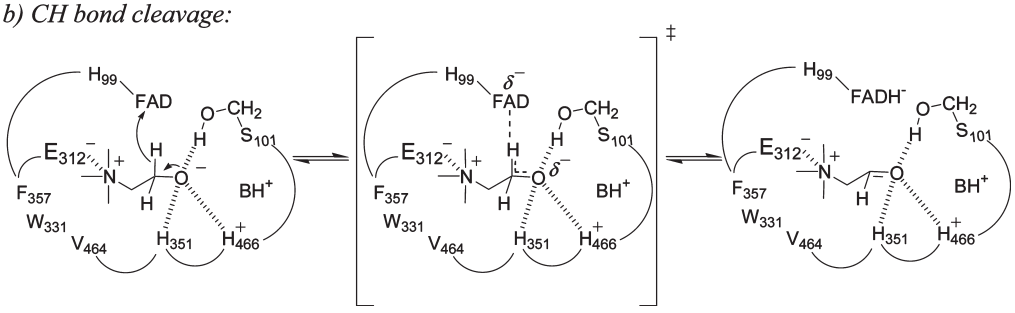

[a]Other residues roles are E312 [substrate binding (*15*)], H351 [hydrogen bonding O atom of the substrate (*29*)], and H466 [electrostatic stabilization of alkoxide species (*34*)].

capability that facilitates the transfer of the hydride ion from the activated alkoxide to the flavin (Scheme 3). Evidence of this conclusion comes from a plot of log(k_5) as a function of the hydrophobicity of residue 101, showing a linear decrease over 4 orders of magnitude of the rate constant for hydride transfer with the decreasing hydrophilicity of residue 101 (Figure 6). Possible steric effects can be immediately ruled out as being responsible for the decrease in the k_5 values because no correlation was found when log(k_5) or k_5 itself was plotted as a function of the volume of the side chain of residue 101 (data not shown). Among the various hydrophobicity scales that are available, the best correlation was found by using the GES scale (R^2 = 0.91), where the hydrophobicity of the amino acid side chains is defined by the free energy for transfer of the amino acid from water to an organic solvent while taking into account the hydrogen bonding ability of the amino acid side chains (*38*). Interestingly, a significantly improved fit of the data was obtained when the Ser101Ala enzyme was excluded (R^2 = 0.99), with the latter enzyme displaying a k_5 value 8 times larger than the value expected from the fit of the data obtained with the other four enzymes (Figure S1 of the Supporting Information). For comparison, R^2 values of 0.75 (with data for Ala101) and 0.87 (without data for Ala101) were obtained using the more popular Kyte hydrophobicity scale (Figures S2 and S3 of the Supporting Information), where hydrophobicity is defined by the free energy for the transfer from water to the vapor phase (*39*). These observations collectively suggest that besides its hydrophilic character, and irrespective of whether the redox potential of the flavin is affected by the substitution, the hydrogen bonding capability of the side chain of residue 101 is also important for the hydride transfer reaction catalyzed by choline oxidase. The presence of a somewhat mobile water molecule in place of the less mobile side chain on the Ser101Ala enzyme would readily explain why the hydride transfer reaction is significantly faster in the Ser101Ala enzyme.

Alkoxide Intermediate versus Transition State. In the Ser101 mutant enzymes, the alkoxide intermediate promotes

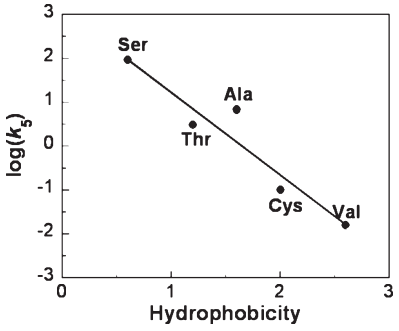

FIGURE 6: Dependence of the rate constant for hydride ion transfer on the hydrophobicity of the amino acid residue at position 101 in choline oxidase. The GES scale for hydrophobicity was used (*38*).

detectable perturbations in the absorbance spectrum of the enzyme-bound flavin, as indicated by the decreased intensity at 450 nm ensuing in the fast kinetic phase of the stopped-flow traces.[3] A previous study showed that another variant of choline oxidase with the active site Asn510 substituted with histidine also catalyzes a stepwise oxidation of choline with cleavage of the O−H and C−H bonds occurring in the time frame of the stopped-flow spectrophotometer (*30*). However, in that case, anaerobic reduction of the flavin was monophasic and the stepwise timing for the cleavages of the O−H and C−H bonds of choline could be

[3]The decrease in absorbance at 450 nm that is associated with the cleavage of the substrate O−H bond (Figure 2A) is too large to be ascribed to the mere presence of the negatively charged alkoxide intermediate close to the flavin in the active site of the enzymes mutated at Ser101. Indeed, cleavage of the O−H bond of choline did not result in absorbance changes of the type reported here in both the wild type and a mutant form of choline oxidase in which Asn510 is replaced with His (*20*, *30*). A spectroscopic characterization of the enzyme−alkoxide intermediate in the reaction catalyzed by the Ser101 mutant enzymes currently aims to elucidate the biophysical rationale for such a significant change in the absorbance of the oxidized enzyme−alkoxide intermediate complex. This will be presented in a separate study.

Scheme A1

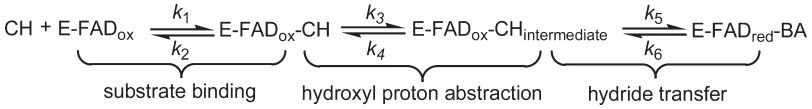

established only by using substrate and solvent KIEs (*30*). A ready explanation for this apparent incongruence is that in the Ser101 mutant enzymes the alkoxide formed in catalysis is a stable reaction intermediate. In contrast, in the reaction of choline oxidation catalyzed by the Asn510His enzyme, the alkoxide is a transition state. The former, being long-lived and stable, would be detected spectrophotometrically within the time frame of the stopped-flow spectrophotometer, whereas the latter would be undetectable with probes other than KIEs because of its lifetime (10^{-12} s).

Implications for Hydride Transfer Reactions Catalyzed by Flavin-Dependent Enzymes. Several flavin-dependent enzymes have in their active sites either a serine, threonine, or tyrosine in a position that is similar, if not equivalent, to that of Ser101 of choline oxidase. Examples include, but are not limited to, class 2 dihydroorotate dehydrogenase (*40*), pyranose 2-oxidase (*41*), glucose oxidase (*42*), nitric oxide synthase (*43*), the old yellow enzyme (*44*), NADPH-cytochrome P450 oxidoreductase (*45*), alditol oxidase (*46*), UDP-galactose 4-epimerase (*47*), cholesterol oxidase (*48*), nitronate monooxygenase (*49*), and heterotetrameric sarcosine oxidase (*50*). In many instances, crystallographic or site-directed mutagenesis studies have suggested that the active site serine, threonine, or tyrosine residues are important for catalysis because they form hydrogen bonds to either the O(4) or N(5) atom of the flavin (*42*−*44*, *46*, *48*, *50*), the substrate in the enzyme−substrate complex (*41*, *47*), or the transition state (*45*) for the reaction catalyzed. The only case in the literature for which multiple substitutions of an active site threonine (i.e., Thr178) equivalent to Ser101 of choline oxidase were engineered and the effects of the substitutions on the rate constant for the hydride transfer reaction were investigated in a stopped-flow spectrophotometer is class 2 dihydroorotate dehydrogenase (*40*). Interestingly, a plot of log(k_{red}) as a function of the hydrophobicity of residue 178 shows that the rate constant for the hydride transfer reaction catalyzed by class 2 dihydroorotate dehydrogenase increases with the increasing hydrophilicity of residue 178 (Figure S4 of the Supporting Information), like the case presented here for choline oxidase. With dihydroorotate dehydrogenase, however, the slope of the line that fits the data to a GES hydrophobicity scale is shallower than that with choline oxidase, e.g., −0.36 ± 0.05 as compared to −1.9 ± 0.3. This suggests that the conclusions that are drawn in our study of choline oxidase, most likely in combination with other features such as the ability of the hydroxyl side chain to form a hydrogen bond to the 7,8-dimethylisoalloxazine of the flavin, may have general relevance for those flavin-dependent enzymes that utilize a hydride transfer mechanism for the oxidation of their organic substrate.

Conclusions. In summary, the results presented in this study for the choline oxidase variants in which serine at position 101 was replaced with alanine, cysteine, threonine, and valine support the conclusions that Ser101 is important for both the activation of the alcohol substrate and the subsequent hydride transfer reaction catalyzed by the enzyme. This is likely exerted by the side chain of residue 101 acting as a hydrogen bond donor to the oxygen atom of the alcohol substrate and of the alkoxide intermediate. This study represents the first instance in which the hydrophilic character of the serine residue proximal to the C(4a) and N(5) flavin atoms in a flavin-dependent enzyme, besides its hydrogen bonding capability, has been shown to be important for efficient transfer of a hydride from the substrate to the enzyme-bound flavin. Analysis of published data for class 2 dihydroorotate dehydrogenase indicates that the hydrophilic character of Thr178 is also important for the hydride transfer reaction catalyzed by that enzyme. In the future, it would be interesting to complement these experimental findings with computational approaches to provide a physical rationale for these conclusions.

APPENDIX

The proposed mechanism for the reaction catalyzed by the choline oxidase Ser101 variant is described. The derivation of the equation that describes the rate of cleavage of the O−H bond and the C−H bond of the substrate follows the logic described by Bernasconi (*51*) and the method by Chaiyen (*52*).

In Scheme A1, E-FAD$_{OX}$ represents oxidized choline oxidase, CH is the substrate choline, BA represents bataine aldehyde, E-FAD$_{red}$ is reduced choline oxidase, and k_1−k_6 are the rate constants. The binding step is in rapid equilibrium; therefore, k_{obs0} is very large and in the dead time of the system, and we cannot measure it.

$$\frac{d\Delta C_{intermediate}}{dt} = k_3\Delta C_{E\text{-}FAD_{ox}\text{-}CH} - (k_4 + k_5)\Delta C_{intermediate} + k_6 C_{E\text{-}FAD_{red}\text{-}BA}\Delta C_{E\text{-}FAD_{red}\text{-}BA} \quad (A1)$$

Because

$$\Delta C_{E\text{-}FAD_{ox}\text{-}CH} = \frac{k_1 C_{CH}\Delta C_{CH}}{k_2} \quad (A2)$$

$$\Delta C_{CH} + \Delta C_{E\text{-}FAD_{ox}\text{-}CH} + \Delta C_{intermediate} + \Delta C_{E\text{-}FAD_{red}\text{-}BA} = 0 \quad (A3)$$

Therefore

$$\Delta C_{E\text{-}FAD_{ox}\text{-}CH} = [k_1 C_{CH}(-\Delta C_{E\text{-}FAD_{ox}\text{-}CH} - \Delta C_{intermediate} - \Delta C_{E\text{-}FAD_{red}\text{-}BA})]/k_2$$

$$\Delta C_{E\text{-}FAD_{ox}\text{-}CH} = \frac{k_1 C_{CH}(\Delta C_{intermediate} + \Delta C_{E\text{-}FAD_{red}\text{-}BA})}{k_2 + k_1 C_{CH}}$$

Replace the $\Delta C_{E\text{-}FAD_{ox}\text{-}CH}$ in eq 1

$$\frac{d\Delta C_{intermediate}}{dt} = -\left(\frac{k_1 k_3 C_{CH}}{k_2 + k_1 C_{CH}} + k_4 + k_5\right)\Delta C_{intermediate} - \left(\frac{k_1 k_3 C_{CH}}{k_2 + k_1 C_{CH}} - k_6 C_{E\text{-}FAD_{red}\text{-}BA}\right)\Delta C_{E\text{-}FAD_{red}\text{-}BA}$$

$$\frac{d\Delta C_{E\text{-}FAD\text{-}BA}}{dt} = k_5\Delta C_{intermediate} - k_6 C_{E\text{-}FAD_{red}\text{-}BA}\Delta C_{E\text{-}FAD_{red}\text{-}BA}$$

On the basis of the logic described by Bernasconi (*51*), let $a_{11} = (k_1k_3C_{CH})/(k_2 + k_1C_{CH}) + k_4 + k_5$, $a_{12} = (k_1k_3C_{CH})/(k_2 + k_1C_{CH}) - k_6C_{E\text{-}FAD_{red}\text{-}BA}$, $a_{21} = k_5$, $a_{22} = k_6C_{E\text{-}FAD_{red}\text{-}BA}$, $x_1 = \Delta C_{intermediate}$, and $x_2 = \Delta C_{E\text{-}FAD_{red}\text{-}BA}$

$$\begin{vmatrix} a_{11} - k_{obs} & a_{12} \\ a_{21} & a_{22} - k_{obs} \end{vmatrix}$$

So

$$k_{obs1} = \frac{1}{2}(a_{11} + a_{22}) + \sqrt{\left[\frac{1}{2}(a_{11}+a_{22})\right]^2 + a_{12}a_{21} - a_{11}a_{22}}$$

$$k_{obs2} = \frac{1}{2}(a_{11} + a_{22}) - \sqrt{\left[\frac{1}{2}(a_{11}+a_{22})\right]^2 + a_{12}a_{21} - a_{11}a_{22}}$$

By taking the sum and the product

$$A = k_{obs1} + k_{obs2} = a_{11} + a_{22}$$

$$= \frac{k_1k_3S}{k_2 + k_1S} + k_4 + k_5 + k_6C_{E\text{-}FAD_{red}\text{-}BA}$$

$$B = k_{obs1}k_{obs2} = a_{11}a_{22} - a_{12}a_{21}$$

$$= \frac{k_1k_3S}{k_2 + k_1S}(k_5 + k_6C_{E\text{-}FAD_{red}\text{-}BA}) + k_4k_6C_{E\text{-}FAD_{red}\text{-}BA}$$

The extrapolation to the origin of the curve fitting of the kinetic data on the dependence of the k_{obs2} value as a function of the substrate concentration in Figures 2B, 3B, and 4B establishes that the kinetic step k_6 is close to zero (*53*).

$$A = k_{obs1} + k_{obs2} = \frac{k_1k_3S}{k_2 + k_1S} + k_4 + k_5$$

So

$$B = k_{obs1}k_{obs2} = \frac{k_1k_3k_5S}{k_2 + k_1S}$$

Substitute $k_{obs1} = A - k_{obs2}$ into B to obtain

$$-k_{obs2}^2 + k_{obs2}A - B = 0$$

$$k_{obs2} = \frac{A \pm \sqrt{A^2 - 4B}}{2} = \frac{A}{2} \pm \frac{A}{2}\sqrt{1 - \frac{4B}{A^2}}$$

While $A^2 \geq 4B$

$$\sqrt{1 - \frac{4B}{A^2}} \approx 1 - \frac{2B}{A^2}$$

Therefore, $k_{obs2} = A - B/A$ or B/A, and $k_{obs1} = B/A$ or $A - B/A$.

Because $k_{obs1} > k_{obs2}$

$$k_{obs2} = \frac{B}{A} = \frac{k_1k_3k_5S}{k_1k_3S + k_1k_4S + k_1k_5S + k_2(k_4 + k_5)}$$

$$= \frac{\frac{k_3k_5}{k_3 + k_4 + k_5}S}{S + \frac{k_2(k_4 + k_5)}{k_1(k_3 + k_4 + k_5)}}$$

So

$$k_{lim2} = \frac{k_3k_5}{k_3 + k_4 + k_5},\ K_{slow} = \frac{k_2(k_4 + k_5)}{k_1(k_3 + k_4 + k_5)}$$

$$k_{obs1} = \frac{B}{k_{obs2}} = \frac{k_1k_3k_5S}{k_2 + k_1S} \times \frac{k_1(k_3 + k_4 + k_5)S + k_2(k_4 + k_5)}{k_1k_3k_5S}$$

$$= \frac{k_1(k_3 + k_4 + k_5)S + k_2(k_4 + k_5)}{k_1S + k_2}$$

$$= \frac{(k_3 + k_4 + k_5)S + \frac{k_2}{k_1}(k_4 + k_5)}{S + \frac{k_2}{k_1}}$$

So

$$k_{lim1} = k_3 + k_4 + k_5,\ K_{fast} = \frac{k_2}{k_1}$$

ACKNOWLEDGMENT

We thank Prof. Dabney W. Dixon for insightful discussions about hydrophobicity scales and Prof. Donald Hamelberg for insightful discussions.

SUPPORTING INFORMATION AVAILABLE

Supplementary Figures S1−S4. This material is available free of charge via the Internet at http://pubs.acs.org.

REFERENCES

1. Gadda, G. (2008) Hydride transfer made easy in the reaction of alcohol oxidation catalyzed by flavin-dependent oxidases. *Biochemistry 47*, 13745–13753.
2. Vilhelmsson, O., and Miller, K. J. (2002) Humectant permeability influences growth and compatible solute uptake by *Staphylococcus aureus* subjected to osmotic stress. *J. Food Prot. 65*, 1008–1015.
3. Peddie, B. A., Wong-She, J., Randall, K., Lever, M., and Chambers, S. T. (1998) Osmoprotective properties and accumulation of betaine analogues by *Staphylococcus aureus*. *FEMS Microbiol. Lett. 160*, 25–30.
4. Peddie, B. A., Chambers, S. T., and Lever, M. (1996) Is the ability of urinary tract pathogens to accumulate glycine betaine a factor in the virulence of pathogenic strains? *J. Lab. Clin. Med. 128*, 417–422.
5. Sakamoto, A., Alia, and Murata, N. (1998) Metabolic engineering of rice leading to biosynthesis of glycine betaine and tolerance to salt and cold. *Plant Mol. Biol. 38*, 1011–1019.
6. Papageorgiou, G. C., and Murata, N. (1995) The unusually strong stabilizing effects of glycine betaine on the structure and function of the oxygen-evolving photosystem II complex. *Photosynth. Res. 44*, 243–252.
7. Alia, Hayashi, H., Sakamoto, A., and Murata, N. (1998) Enhancement of the tolerance of *Arabidopsis* to high temperatures by genetic engineering of the synthesis of glycine betaine. *Plant J. 16*, 155–161.
8. Alia, Kondo, Y., Sakamoto, A., Nonaka, H., Hayashi, H., Saradhi, P. P., Chen, T. H., and Murata, N. (1999) Enhanced tolerance to light stress of transgenic *Arabidopsis* plants that express the *codA* gene for a bacterial choline oxidase. *Plant Mol. Biol. 40*, 279–288.
9. Sakamoto, A., Valverde, R., Alia, Chen, T. H., and Murata, N. (2000) Transformation of *Arabidopsis* with the *codA* gene for choline oxidase enhances freezing tolerance of plants. *Plant J. 22*, 449–453.
10. Andresen, P. A., Kaasen, I., Styrvold, O. B., Boulnois, G., and Strom, A. R. (1988) Molecular cloning, physical mapping and expression of the bet genes governing the osmoregulatory choline-glycine betaine pathway of *Escherichia coli*. *J. Gen. Microbiol. 134*, 1737–1746.
11. Ghanem, M., Fan, F., Francis, K., and Gadda, G. (2003) Spectroscopic and kinetic properties of recombinant choline oxidase from *Arthrobacter globiformis*. *Biochemistry 42*, 15179–15188.
12. Fan, F., Ghanem, M., and Gadda, G. (2004) Cloning, sequence analysis, and purification of choline oxidase from *Arthrobacter globiformis*: A bacterial enzyme involved in osmotic stress tolerance. *Arch. Biochem. Biophys. 421*, 149–158.

13. Ghanem, M., and Gadda, G. (2006) Effects of reversing the protein positive charge in the proximity of the flavin N(1) locus of choline oxidase. *Biochemistry 45*, 3437–3447.
14. Hoang, J. V., and Gadda, G. (2007) Trapping choline oxidase in a nonfunctional conformation by freezing at low pH. *Proteins 66*, 611–620.
15. Quaye, O., Lountos, G. T., Fan, F., Orville, A. M., and Gadda, G. (2008) Role of Glu312 in binding and positioning of the substrate for the hydride transfer reaction in choline oxidase. *Biochemistry 47*, 243–256.
16. Orville, A. M., Lountos, G. T., Finnegan, S., Gadda, G., and Prabhakar, R. (2009) Crystallographic, spectroscopic, and computational analysis of a flavin C4a-oxygen adduct in choline oxidase. *Biochemistry 48*, 720–728.
17. Gadda, G. (2003) pH and deuterium kinetic isotope effects studies on the oxidation of choline to betaine-aldehyde catalyzed by choline oxidase. *Biochim. Biophys. Acta 1650*, 4–9.
18. Gadda, G. (2003) Kinetic mechanism of choline oxidase from *Arthrobacter globiformis*. *Biochim. Biophys. Acta 1646*, 112–118.
19. Gadda, G., Powell, N. L., and Menon, P. (2004) The trimethylammonium headgroup of choline is a major determinant for substrate binding and specificity in choline oxidase. *Arch. Biochem. Biophys. 430*, 264–273.
20. Fan, F., and Gadda, G. (2005) On the catalytic mechanism of choline oxidase. *J. Am. Chem. Soc. 127*, 2067–2074.
21. Fan, F., and Gadda, G. (2005) Oxygen- and temperature-dependent kinetic isotope effects in choline oxidase: Correlating reversible hydride transfer with environmentally enhanced tunneling. *J. Am. Chem. Soc. 127*, 17954–17961.
22. Fan, F., Germann, M. W., and Gadda, G. (2006) Mechanistic studies of choline oxidase with betaine aldehyde and its isosteric analogue 3,3-dimethylbutyraldehyde. *Biochemistry 45*, 1979–1986.
23. Gadda, G., Fan, F., and Hoang, J. V. (2006) On the contribution of the positively charged headgroup of choline to substrate binding and catalysis in the reaction catalyzed by choline oxidase. *Arch. Biochem. Biophys. 451*, 182–187.
24. Fan, F., and Gadda, G. (2007) An internal equilibrium preorganizes the enzyme-substrate complex for hydride tunneling in choline oxidase. *Biochemistry 46*, 6402–6408.
25. Xin, Y., Gadda, G., and Hamelberg, D. (2009) The cluster of hydrophobic residues controls the entrance to the active site of choline oxidase. *Biochemistry 48*, 9599–9605.
26. Quaye, O., and Gadda, G. (2009) Effect of a conservative mutation of an active site residue involved in substrate binding on the hydride tunneling reaction catalyzed by choline oxidase. *Arch. Biochem. Biophys. 489*, 10–14.
27. Quaye, O., Cowins, S., and Gadda, G. (2009) Contribution of flavin covalent linkage with histidine 99 to the reaction catalyzed by choline oxidase. *J. Biol. Chem. 284*, 16990–16997.
28. Quaye, O., Nguyen, T., Gannavaram, S., Pennati, A., and Gadda, G. (2010) Rescuing of the hydride transfer reaction in the Glu312Asp variant of choline oxidase by a substrate analogue. *Arch. Biochem. Biophys. 499*, 1–5.
29. Rungsrisuriyachai, K., and Gadda, G. (2008) On the role of histidine 351 in the reaction of alcohol oxidation catalyzed by choline oxidase. *Biochemistry 47*, 6762–6769.
30. Rungsrisuriyachai, K., and Gadda, G. (2010) Role of asparagine 510 in the relative timing of substrate bond cleavages in the reaction catalyzed by choline oxidase. *Biochemistry 49*, 2483–2490.
31. Finnegan, S., and Gadda, G. (2008) Substitution of an active site valine uncovers a kinetically slow equilibrium between competent and incompetent forms of choline oxidase. *Biochemistry 47*, 13850–13861.
32. Finnegan, S., Agniswamy, J., Weber, I. T., and Gadda, G. (2010) Role of valine 464 in the flavin oxidation reaction catalyzed by choline oxidase. *Biochemistry 49*, 2952–2961.
33. Finnegan, S., Yuan, H., Wang, Y. F., Orville, A. M., Weber, I. T., and Gadda, G. (2010) Structural and kinetic studies on the Ser101Ala variant of choline oxidase: Catalysis by compromise. *Arch. Biochem. Biophys. 501*, 207–213.
34. Ghanem, M., and Gadda, G. (2005) On the catalytic role of the conserved active site residue His466 of choline oxidase. *Biochemistry 44*, 893–904.
35. Schowen, K. B., and Schowen, R. L. (1982) Solvent isotope effects of enzyme systems. *Methods Enzymol. 87*, 551–606.
36. Kirinčič, S., and Klofutar, C. (1999) Viscosity of aqueous solutions of poly(ethylene glycol)s at 298.15 K. *Fluid Phase Equilib. 115*, 311–325.
37. Cook, P. F., and Cleland, W. W. (2007) Enzyme Kinetics and Mechanism, Garland Science, New York.
38. Engelman, D. M., Steitz, T. A., and Goldman, A. (1986) Identifying nonpolar transbilayer helices in amino acid sequences of membrane proteins. *Annu. Rev. Biophys. Biophys. Chem. 15*, 321–353.
39. Kyte, J., and Doolittle, R. F. (1982) A simple method for displaying the hydropathic character of a protein. *J. Mol. Biol. 157*, 105–132.
40. Kow, R. L., Whicher, J. R., McDonald, C. A., Palfey, B. A., and Fagan, R. L. (2009) Disruption of the proton relay network in the class 2 dihydroorotate dehydrogenase from *Escherichia coli*. *Biochemistry 48*, 9801–9809.
41. Pitsawong, W., Sucharitakul, J., Prongjit, M., Tan, T. C., Spadiut, O., Haltrich, D., Divne, C., and Chaiyen, P. (2010) A conserved active-site threonine is important for both sugar and flavin oxidations of pyranose 2-oxidase. *J. Biol. Chem. 285*, 9697–9705.
42. Wohlfahrt, G., Witt, S., Hendle, J., Schomburg, D., Kalisz, H. M., and Hecht, H. J. (1999) 1.8 and 1.9 Å resolution structures of the *Penicillium amagasakiense* and *Aspergillus niger* glucose oxidases as a basis for modelling substrate complexes. *Acta Crystallogr. D55*, 969–977.
43. Panda, S. P., Gao, Y. T., Roman, L. J., Martasek, P., Salerno, J. C., and Masters, B. S. (2006) The role of a conserved serine residue within hydrogen bonding distance of FAD in redox properties and the modulation of catalysis by Ca^{2+}/calmodulin of constitutive nitric-oxide synthases. *J. Biol. Chem. 281*, 34246–34257.
44. Xu, D., Kohli, R. M., and Massey, V. (1999) The role of threonine 37 in flavin reactivity of the old yellow enzyme. *Proc. Natl. Acad. Sci. U. S.A. 96*, 3556–3561.
45. Shen, A. L., and Kasper, C. B. (1996) Role of Ser457 of NADPH-cytochrome P450 oxidoreductase in catalysis and control of FAD oxidation-reduction potential. *Biochemistry 35*, 9451–9459.
46. Forneris, F., Heuts, D. P., Delvecchio, M., Rovida, S., Fraaije, M. W., and Mattevi, A. (2008) Structural analysis of the catalytic mechanism and stereoselectivity in *Streptomyces coelicolor* alditol oxidase. *Biochemistry 47*, 978–985.
47. Liu, Y., Thoden, J. B., Kim, J., Berger, E., Gulick, A. M., Ruzicka, F. J., Holden, H. M., and Frey, P. A. (1997) Mechanistic roles of tyrosine 149 and serine 124 in UDP-galactose 4-epimerase from *Escherichia coli*. *Biochemistry 36*, 10675–10684.
48. Lyubimov, A. Y., Lario, P. I., Moustafa, I., and Vrielink, A. (2006) Atomic resolution crystallography reveals how changes in pH shape the protein microenvironment. *Nat. Chem. Biol. 2*, 259–264.
49. Ha, J. Y., Min, J. Y., Lee, S. K., Kim, H. S., Kim do, J., Kim, K. H., Lee, H. H., Kim, H. K., Yoon, H. J., and Suh, S. W. (2006) Crystal structure of 2-nitropropane dioxygenase complexed with FMN and substrate. Identification of the catalytic base. *J. Biol. Chem. 281*, 18660–18667.
50. Chen, Z. W., Hassan-Abdulah, A., Zhao, G., Jorns, M. S., and Mathews, F. S. (2006) Heterotetrameric sarcosine oxidase: Structure of a diflavin metalloenzyme at 1.85 Å resolution. *J. Mol. Biol. 360*, 1000–1018.
51. Bernasconi, C. (1976) Relaxation kinetics, Academic Press, New York.
52. Sucharitakul, J., Prongjit, M., Haltrich, D., and Chaiyen, P. (2008) Detection of a C4a-hydroperoxyflavin intermediate in the reaction of a flavoprotein oxidase. *Biochemistry 47*, 8485–8490.
53. Strickland, S., Palmer, G., and Massey, V. (1975) Determination of dissociation constants and specific rate constants of enzyme-substrate (or protein-ligand) interactions from rapid reaction kinetic data. *J. Biol. Chem. 250*, 4048–4052.